We are IntechOpen,
the world's leading publisher of
Open Access books
Built by scientists, for scientists

5,800
Open access books available

142,000
International authors and editors

180M
Downloads

Our authors are among the

154
Countries delivered to

TOP 1%
most cited scientists

12.2%
Contributors from top 500 universities

CLARIVATE ANALYTICS

**BOOK
CITATION
INDEX**

INDEXED

WEB OF SCIENCE™

Selection of our books indexed in the Book Citation Index
in Web of Science™ Core Collection (BKCI)

Interested in publishing with us?
Contact book.department@intechopen.com

Chapter

Experimental Studies of Asynchronous Electric Drives with "Stepwise" Changes in the Active Load

Vladimir L. Kodkin, Alexandr S. Anikin,
Alexandr A. Baldenkov and Natalia A. Loginova

Abstract

The article offers the results of experimental studies of asynchronous electric 10 motors with "squirrel cage" rotor with frequency control. The results of bench tests of the modes of parrying stepwise changes in the load created by a similar frequency-controlled electric drive are presented. A preliminary qualitative analysis of the known control methods is carried out and it is shown that the assumptions made when creating their algorithms in the modes of countering the load become too significant. The reasons for this are the fundamental inaccuracies of the vector equations of asynchronous electric motors with frequency regulation. The proposed interpretation of asynchronous electric motors by nonlinear continuous transfer functions, outlined in the articles written by the same authors earlier, and the corrections they proposed turned out to be more accurate for the operating modes under consideration than the traditional methods of interpretation and correction of the frequency control of asynchronous electric motors This made it possible to assess as objectively as possible the effectiveness of the interpretation of asynchronous electric drives and methods of their regulation. Numerous articles on this topic over the past 25–30 years have not provided such results.

Keywords: asynchronous drive, frequency regulation, dynamic positive feedbacks, active stator current, rotor current, signal spectrum

1. Introduction

The paradoxical situation has developed in the last 20 years in the frequency control asynchronous electric drives.

On the one hand, the frequency control of squirrel cage induction motor (SCIM) with semiconductor frequency and voltage converters (FC) is widespread in industry and energy, has several universal control methods that provide applied in increasingly complex and accurate technological units [1–4].

On the other hand, there are currently several fundamental unresolved theoretical problems that have been formed more than 100 years ago—when forming the theory of AC electrical machines.

The description of the processes of AC electric drives control processes is the vector equations and flowing from them—substitution schemes and vector diagrams (**Figure 1**) ([1], p. 18):

$$u_1 = i_1\left(r_1 + jx_{1\sigma}\right) + ji_m x_m$$

$$0 = i_2\left(\frac{r_2}{s} + jx_{2\sigma}\right) + ji_m + x_m$$

$$m = \frac{m_1}{2}Z_P L_m |i_2 \times i_m| = \frac{m_1}{2}L_m I_{2\,max} I_{m\;max} sin\psi \qquad (1)$$

$$x_1 = \omega_1 L_1; x_2 = \omega_1 L_2; x_m = \omega_1 L_m$$

These equations have a number of assumptions and simplifications acceptable to static modes, but completely erroneous for dynamic.

First, these equations suggest the sinusoidal nature of currents and stresses formed in asynchronous electric motors. The theory of control that operates vectors is simply not able to take into account any more components of these variables. At the same time, the presence of such components—the so-called "higher harmonics" in the currents of the motors and FC recognize all experts. However, in the engine equation, these components are not included, and only electrical interference is taken into account from all problems.

Secondly, the operating vectors instead of sinusoidal functions, interpreting currents in the stator and the rotor of the engines are valid only if the frequencies of their change are constant. Only in this case the differential equations "pass" in the vector and can be significantly simplified. It is important to note that even evaluating the error of such a replacement during frequency variations is analytically very difficult.
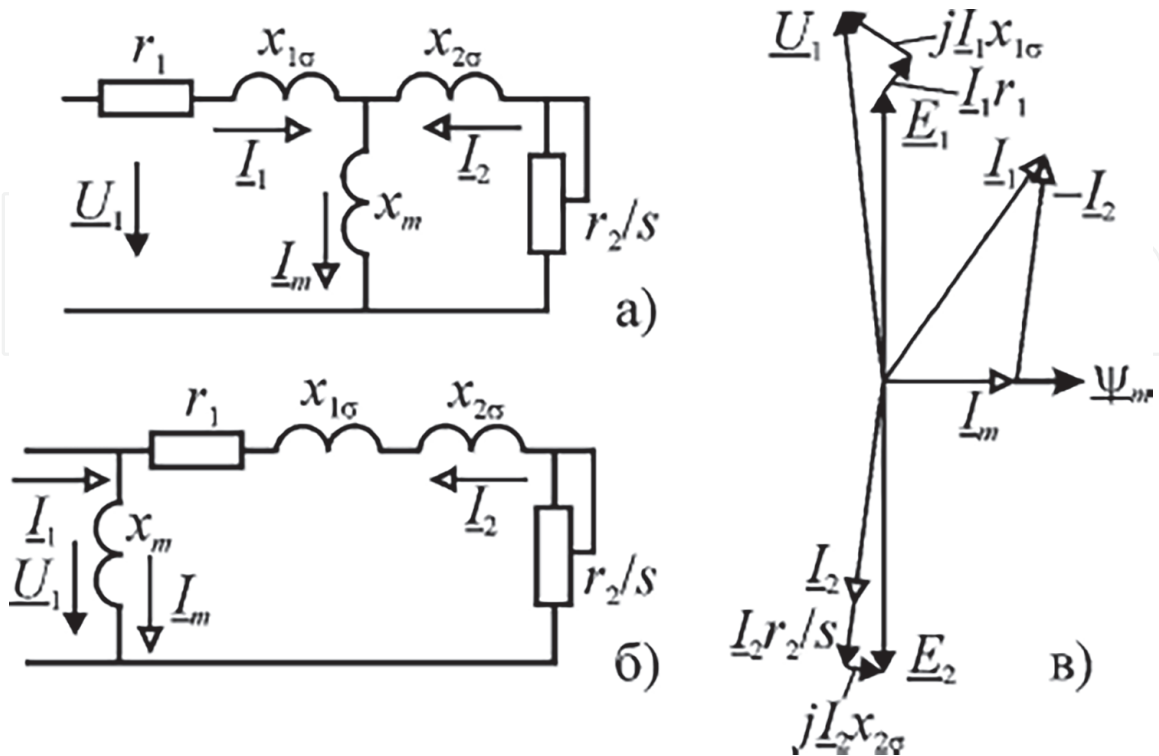

Figure 1.
Substitution scheme, vector diagram of asynchronous motor and vector equations in traditional form [1].
X$_1$, X$_2$ – inductive resistances stator and rotor; r$_1$, r$_2$ – active resistances stator and rotor; I$_1$, I$_2$ – stator and rotor currents; and E$_2$, U$_1$ – rotor EMF and stator voltage.

Thirdly, even with these assumptions of the equation remain extremely nonlinear and complex. In compiling the equations of elements of the vector control unit, additional simplifications are assumed, for example—the constancy of the rotor magnetic flux and the equality of the frequency of the stator voltage and the speed of rotation.

"The coordinate junction block (CJB) can be constructed on the basis of the equations of the control model controlled by voltage ([1], p. 2.22). They can be put $\omega_1 = \omega$ and $\frac{d\Psi_2}{dt} = 0$."

Thus, the generally accepted alternating current equations for vector control are largely simplified equations, which, in principle, incorrectly describe transient processes associated with changes in the frequency of stator voltage. Such changes lead to a change in the substitution schemes themselves, because their parameters: $x_1 = \omega_1 L_1; x_2 = \omega_1 L_2; x_m = \omega_1 L_m$ directly depend on the frequency.

The "qualitative processes" of the drive reaction on stepped load jumps can be obtained by combining the calculations of the substitution schemes with the calculations of the mechanical characteristics. If the frequency of the stator voltage does not change, then such descriptions are sufficiently accurate, since only the element $\frac{r_2}{S}$ is changed in such modes in the substitution schemes, and quite quickly. In this case, the initial and final states correspond to two substitution schemes with different $\frac{r_2}{S}$ and, respectively, by different current vectors. But with more complex frequency control algorithms, under which significant changes in the stator voltage occur—amplitude and frequency, new vector diagrams and substitution schemes are "formed" at each moment in which the frequency ω_1 changes. In these cases, high-quality analysis is significantly complicated, since all elements of the substitution scheme change, and the transition from one state to another vector equations is not described in principle. A description of such processes and their correction require a different approach or at least understanding the causes of the problems of existing approaches. This article provides several experiments, the results of which make it possible to understand the processes of stepped load jumps in asynchronous drives with different frequency control methods.

All equations for alternating current machines are designed in the 20s of the last centuries, when adjusting the frequency of the stator voltage was the problem of a distant future. In the past 30 years, this future has come, but simplified remains and make final control errors too significant, and theoretical provisions and even modeling are most often inconclusive. The most significant results of studies of asynchronous electric drives in this situation are experiments, and as close as possible to real industrial conditions.

At the same time, the experiments also require special justifications, since the processes in the asynchronous electric motor rotor are not available for measurement.

This state of affairs restrains the introduction of asynchronous electric drives in new areas for them—in aggregates requiring speed and accuracy. In addition, it is difficult to optimize electric drives in power engineering and transport where they are widely used. At the same time, their economy, acceptable price and high reliability remain a significant cause of research to improve their controllability.

Consider the main generally accepted methods for control of asynchronous electric drives.

2. Formulation of the problem

2.1 Physics of traditional control methods

Scalar control, which is customary to be simple and reliable—at a given speed, the scalar is selected—amplitude and frequency of change of voltage supplied to the

engine stator. Mechanical characteristics are determined by the properties of the electric motor and the dependence $U(f_1)$. The structural scheme in **Figure 2**.

In **Figure 3a** shows the diagrams of the active values of the stator current and speed during acceleration and when the load is signed, obtained during stand-based studies, described in detail several articles [5–7].

The transition trajectory is determined by processes in the motor. Qualitatively these processes are as follows: When exposed to the load torque, the speed of rotation decreases, currents in the rotor and the stator increase, the slip in the motor grows and increases the torque developed by the motor to the state to which the torque corresponds equally to the load. If the parameters of the motor and the substitution schemes are "correct," the process occurs without oscillations and is fast enough, as in the examples of experiments in **Figure 3a**.

In **Figure 3b**, the mechanical characteristics of the motor and the trajectory of the transition from point A (with low load) to point B (with a large load torque).

In **Figure 3c**—the mechanical characteristics of the transition to the mechanical characteristic, corrected IR-compensation during load. Changes in working points B_1 and B are minor.

2.1.1 Vector control sets the task of efficient drive control

To do this, in the models embedded in the control unit of the FC on the measured values of the stator current and stator voltage, the required parameters of the stator voltage vector are calculated, which may vary at any time. The initial engine equations—significantly nonlinear undergo many simplifications, the main of which are the constancy of the rotor flow, the equality of the frequency of the stator speed voltage and the absence of other harmonics [2].
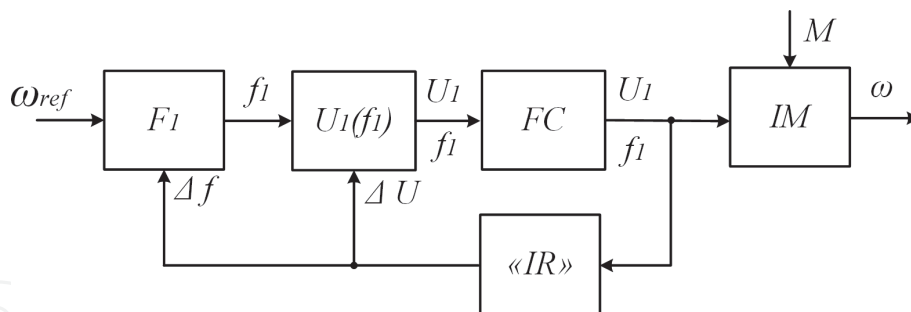

Figure 2.
Structural scheme of asynchronous electric drive with scalar control.
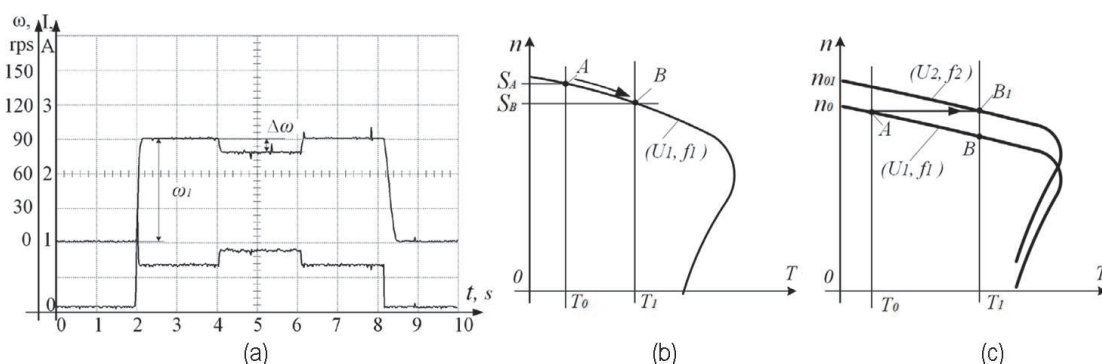

Figure 3.
Process diagrams (a) and mechanical characteristics (b and c) of asynchronous drive with scalar control.

$$\omega_1 = \omega; \frac{d\Psi_2}{dt} = 0 \tag{2}$$

In this case, the algorithm for the control of vector sensorless control picks up the vector of stator voltage, but not the transition path from one vector to another (**Figure 4**).

(Transition trajectories are given special attention in a separate method of vector control—"Direct Torque Control." This method is used mainly by ABB. In the articles dedicated to the method, the algorithms are described mainly at the level of logical provisions. As part of this work, this method of control will be a dedicated comment. Special studies have not been conducted.)

The purpose of the vector control algorithms is to linearize the drive and bring its characteristics to the characteristics of the DC drive characteristics, but the assumptions and errors adopted at these conclusions, as well as the inconsistency of the reality model makes the control error. It should be noted that for linearization, the vector control uses serial corrective devices that do poorly perform these functions. Especially in variations in the characteristics of the linearizable object. "Interferes" into operation and correction and impulse nature of the power of the frequency converter, through which the "correction" of the nonlinearities of the asynchronous electric motor occurs. These features of vector control are noted by almost all researchers [1–4]. In general, in the opening vector control of the change of stator voltage, the load jump is not too large and the processes of the load jump are not much different from the scalar control—**Figures 3c** and **5b**.

Experiments have shown that when overclocking the task signals with a small and unchanged load, assumptions (1) can be considered permissible and the engine equations quite correctly take into account changes in the frequency of the stator voltage and form the correct transition path from the vector state with one frequency to another, but in parrying mode adaptation loads does not occur, the differences in the speed of rotation and frequency of the stator voltage is a significant amount (absolute slip). And the transition trajectory to another state is not corrected. Most often, vector sensorless control poorly adjusts the voltage parameters on the stator and the engine is steaming the load in the same way as with a scalar control mode (**Figure 5a**). Mechanical characteristics are shown in **Figure 5b**. Vector control eliminates unstable "branches" of mechanical characteristics, at the same time, work areas differ little with a scalar. In **Figure 5b** shows the mechanical characteristics of the drives with the reaction to the load diagram and the transition trajectory.

2.1.2 Vector control with a speed loop

By analogy with direct current drives, the additional linearization circuit should carry out the speed control circuit with the PID regulator.
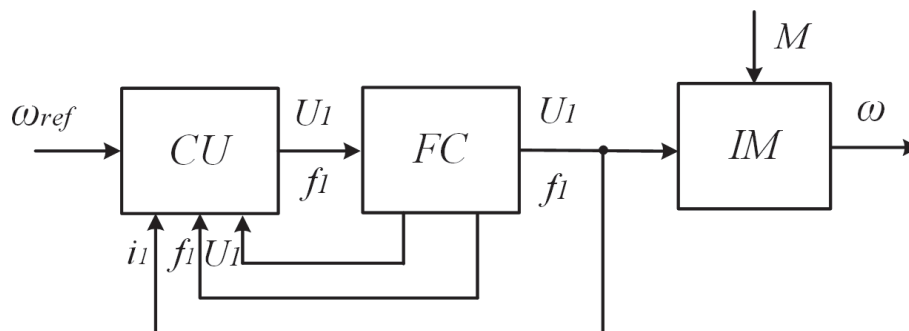

Figure 4.
Structural scheme of asynchronous electric drive with vector sensorless control.
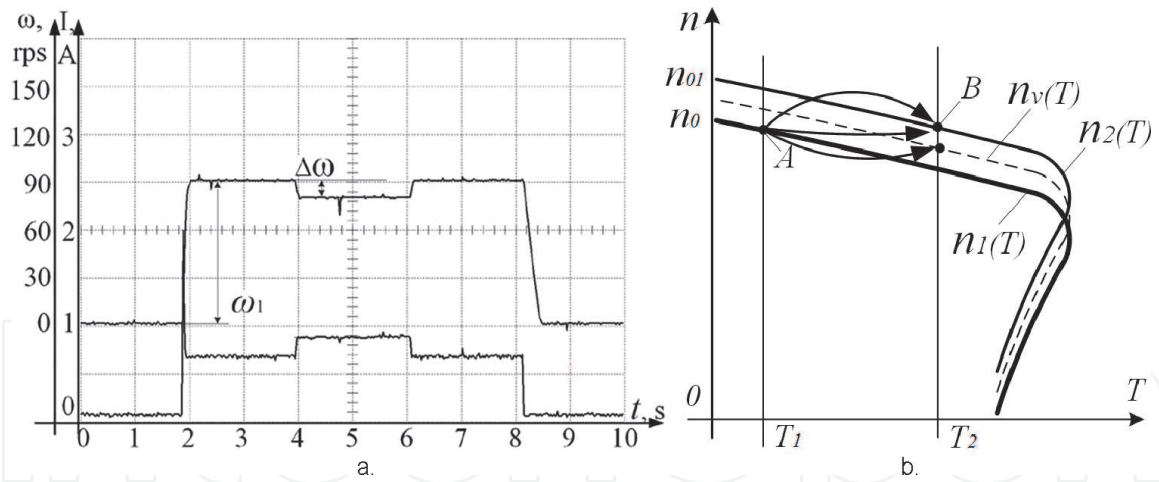
Figure 5.
Process diagrams (a) and mechanical characteristics (b) of asynchronous drive with vector control.

Speed sensors are quite rarely installed on general industrial mechanisms as shown experiments on the stand of a special effect on their application in drives with vector control is not too significant.

When the rotation speed circuit, the control signals for the FC are formed in the PID controller, the inputs of which are sent to the speed of rotation speed and the feedback signal. At the same time, all the problems of dumbfounded vector control are only aggravated (**Figure 6**).

One of the main assumptions of vector sensorless control is the equality of the frequency of the stator voltage and the speed of rotation in the output of the equation coordinate junction block (CJB) of the vector control ([1], p. 61):

$$\omega_1 = \omega \tag{3}$$

When controlling the speed of rotation on the side of the task with the PID controller, this is quite acceptable, but when the loading torque is parried, the permissibility of speed equality and frequency is fundamentally incorrect.

At the time of the jump of load, a dynamic failure of the motor speed occurs, the output of the speed controller generates a signal to an increase in the frequency of the rotor voltage following the conditions (assumptions) in the drive, this leads to a mitigation of the mechanical characteristic (**Figure 7c**), an increase in the dynamic rate of speed and tighten the speedy recovery. This follows from the process diagrams and the transition paths on the graphs of mechanical characteristics (**Figure 5**).

"Double" linearization with very significant assumptions leads to the fact that the acceleration of the drive is similar to the acceleration of the DC drive, and the
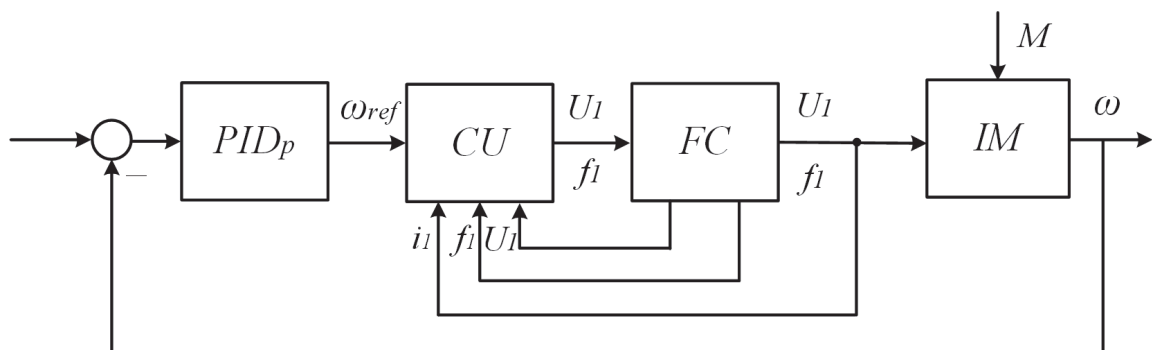

Figure 6.
Structural scheme of asynchronous electric drive with vector sensorless control and speed loop.
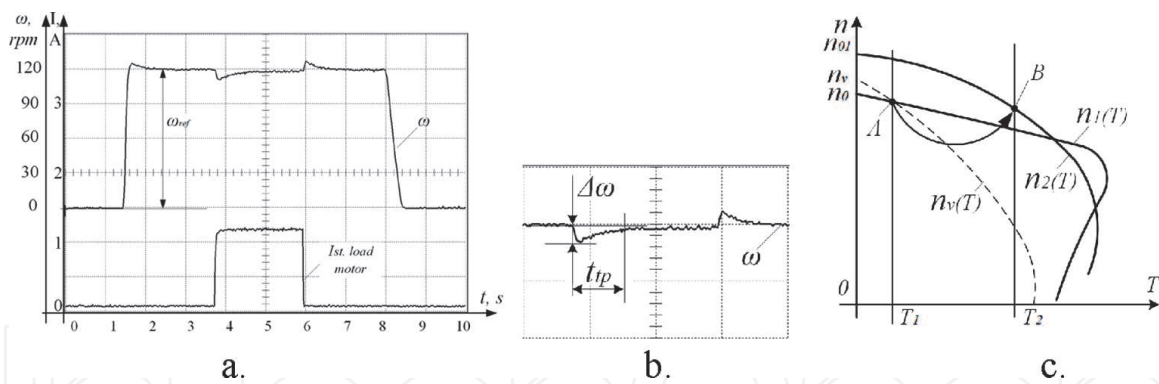
Figure 7.
Process charts (a and b) and mechanical characteristics (c) asynchronous drive with vector control and PID-regulator on speed loop.

processes of parrying the torque load in such a drive have zero static error in speed. However, the efficiency of such a drive cannot be considered significant. The time of the transition process and the dynamic failure of the speed are such that it is impossible to use this option of parrying the load for almost any industrial mechanism.

Comparison of the process of parrying of torques shows that the initial and final states can be the same in the drive, but the transitions between them have an infinite set of trajectories, which are determined by the stator voltage, and the control method form the transition path and the final vector.

2.1.3 Mathematics describing modes of operation

A significant role in the formation of algorithms is played by the mathematics of the description of processes in alternating current electric machines. In describing the operation of the SCIM [2], vector equations and dependencies with a large number of assumptions and simplifications are used.

Vector equations describing all asynchronous and synchronous motors, do not take into account the variable nature of the frequency of voltages and currents. It should be recognized if you assume that the frequency of the stator voltage is a complex function of time, the transition from Eqs. (2.19) to (2.21) ([1], p. 56) will be impossible and, the motor equations are complicated so much to analyze them and choose them effective correction will be impossible.

In the works [5–11], a nonlinear transfer function was proposed linking the mechanical torque developed by the SCIM and the absolute slip—the difference between the frequency of the stator voltage and the speed of rotation of the engine. The formula of this function includes, as variables, the frequency of the stator voltage and the relative slip. The formula can be called a nonlinear transfer function or a dynamic Kloss formula. In the articles [5–8], the conclusion of the proposed nonlinear transfer function is given in sufficient detail, the result is as follows:

$$W(p) = \frac{2M_k(T_2'p+1)S_k}{\omega_1\left[(1+T_2'p)^2S_k^2+\beta^2\right]} \tag{4}$$

where, ω_1 is the frequency of stator voltage, β is a relative slip, depending on the load of the drive.

This gear ratio corresponds to the structural diagram of the SCIM, shown in **Figure 8**.
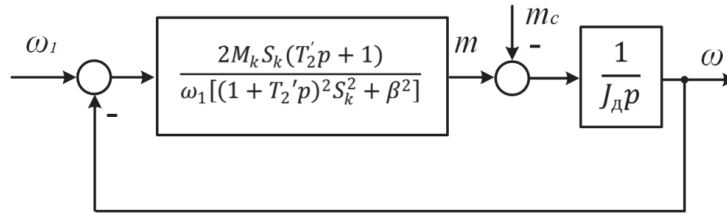
Figure 8.
Block diagram of the ADCZ with a nonlinear transfer function of the link forming the torque.

The works [9–13] show how it is possible to linearize the specified transfer function, that is, to exclude or significantly weaken the dependence of the transfer function and the dynamics of the asynchronous drive on the frequency of the stator voltage and sliding by positive feedback on the developed torque. The block diagram will take the form (**Figure 9**):

The transfer function of the corrective link, which is necessary for positive feedback to maintain the stability of the drive, is as follows:

$$W_{DPF} = \frac{\omega_1 \beta^2}{2M_k S_k (T_2' p + 1)};$$ (5)

The equivalent transfer function of the drive with this connection will take the form:

$$W_{eqv} = \frac{2M_k S_k (T_2' p + 1)}{\omega_1 \left[(1 + T_2' p)^2 S_k^2\right]} = \frac{2M_k}{\omega_1 S_k (1 + T_2' p)}$$ (6)

From the point of view of mathematics, the transfer function with parameters depending on the functions of frequency and slip, this is the same inaccurate mathematical expression, as well as the vector equation, originally derived at unchanged frequencies of harmonic variables—the currents of the engine and EMF rotor and the stator used to analyze the dynamics of these same variables. However, there is one significant difference. If the vector equation is valid exclusively for the constant frequencies of signals associated with the equation, and in principle cannot describe the change in these frequencies, the transfer function retains its ability to describe the dynamics of processes in some area of changes in these functions and even has sufficient accuracy of this description.

So, when the drive is working out a torque disturbance at a constant rotational speed (and a constant frequency of the stator voltage) with a slight (for the transfer function) change in the relative slip β, the transfer function describes the processes quite accurately, and, more importantly, allows you to accurately select corrective connections that linearize the transfer function and make the parrying of the
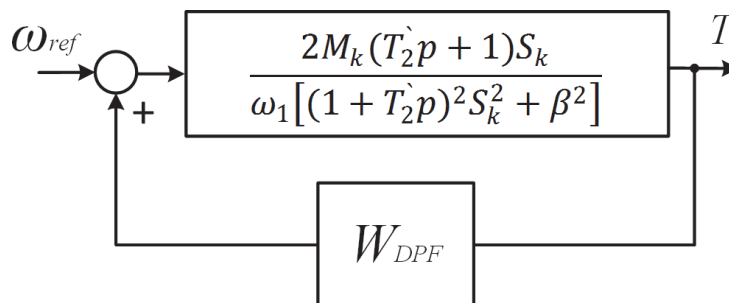
Figure 9.
Block diagram of SCIM with dynamic positive feedback (DPF).

disturbance in the drive much more efficient. So, the proposed positive dynamic feedback by the torque of the engine or its analogue:

$$W_{DPF} = \frac{K}{(T'_2 p + 1)} \qquad (7)$$

The transfer function forms and optimally the transition trajectory and significantly reduces the time of transient processes. Dynamic "dips" speeds are also reduced. Experiments exploring the reaction of the drive to jump of load at various methods of controlling the SCIM fully confirmed this (**Figure 10b**).

The processes in **Figure 10b** show that DPF allows correcting the static error of the drive and significantly speeding up transients. At the same time, the nonlinear transfer function can describe transients and justify continuous devices for their correction, which is the positive feedback on the active component of the stator current. The stator voltage "selected" by this feedback (voltage amplitude and frequency) provides parrying of step loads with minimal transient processes (**Figure 10b**).

This made it possible to formulate a hypothesis that the identification of SCIM with FC a non-linear transfer function is more accurate than vector equations, which is confirmed by the choice of a more effective correction. In asynchronous electric drives using widely used frequency converters, it is quite problematic to introduce positive torque feedback. As experiments have shown [14, 15], it can be replaced by a connection according to the active component of the stator current, which is measured by almost all known frequency converters used in industry.

As mentioned above, the crucial importance in assessing the correctness and effectiveness should be given to experimental studies.

The stand where the research was carried out initially consisted of two identical asynchronous electric drives, each of which contains an asynchronous
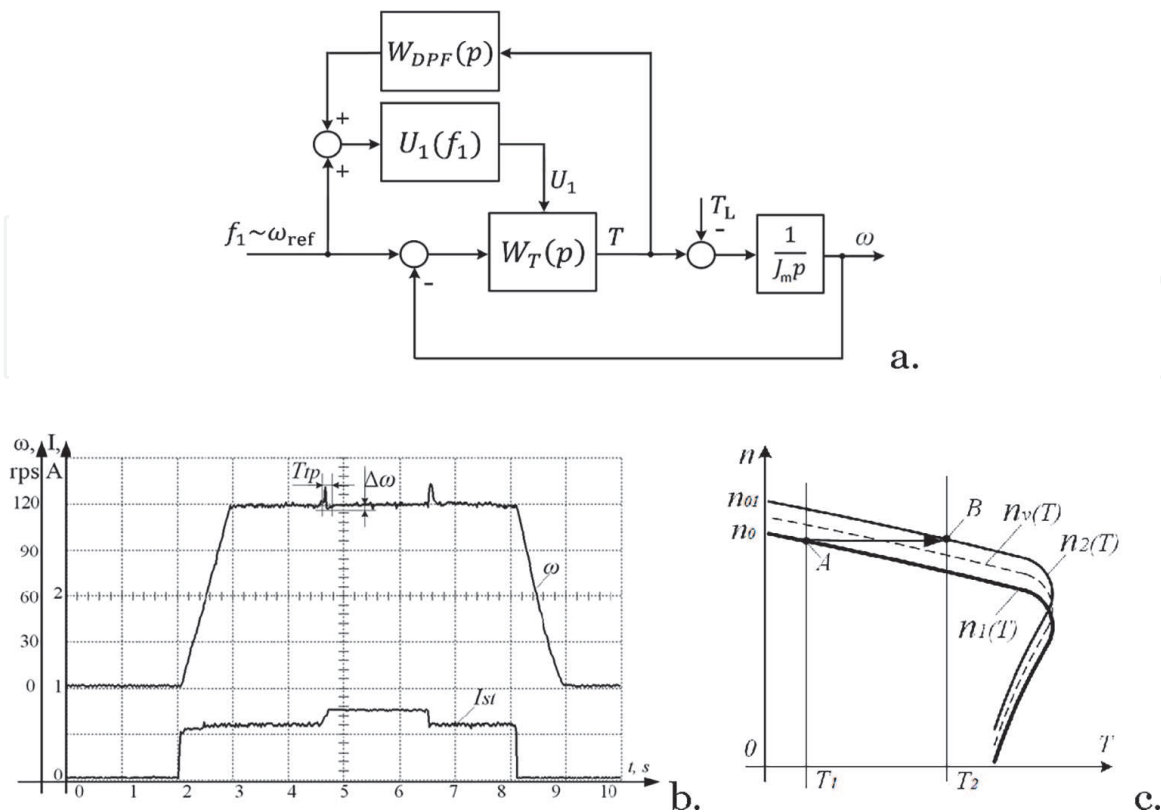

Figure 10.
Structural diagram of the actuator with dynamic bond on time (a), transient processes (b), and mechanical characteristics (c).

short-circuited electric motor and a frequency and voltage converter. The drives operate on one common shaft, the stand contains current sensors and a rotation speed sensor of the common shaft of the motors and a generator of periodic control signals. Quite a lot of different experiments were carried out, described in detail in the articles [16–20].

This study provides the results of experiments during steady-state after the jump of load. These modes of operation are selected, the most exactly corresponding to the vector equations of asynchronous electric drives and well-specific qualitative analysis using well-known methods, mechanical characteristics of the drive (**Figure 11**).

The technology of experiments is extremely simplified. A certain control mode is set in the working drive—vector sensorless or with speed feedback, scalar, or with positive feedback—DPF or DPF2 (DPF2 is a dynamic positive feedback, similar to DPF, but with an increased transmission coefficient ($Kt = 3$)). Scalar control is installed in the load drive. Directly by the signal supplied to the input of the frequency converter *UZ2* of the working motor *M2*, the drive is output to a certain rotation speed (and the corresponding frequency of the stator voltage). After a certain time interval, a task is sent to the frequency converter *UZ1* of the load motor *M1*. The operating mode of the load drive is determined by the task for the speed of rotation, as an equivalent of the mechanical characteristic (**Figure 12**). The drives work counter. The resulting modes are well explained by the mechanical character-istics—**Figure 12**. The working points are determined by the intersection of the mechanical characteristics of the working and load motors. At the same time, **Figure 12a**—U/f = const., **Figure 12b**—$U_2/f_2 > U_1/f_1$.

The jump of load smoothly enough, the rate of load increase is commensurate with the processes of torque formation in the working drive.

The parameters of the modes—the stator currents and the rotation speed (or the sliding value) are determined by the vectors of the stator voltage, which the corresponding control algorithm will "choose." The diagrams of the speed and current of the stator are similar to those shown in **Figures 4–6**.
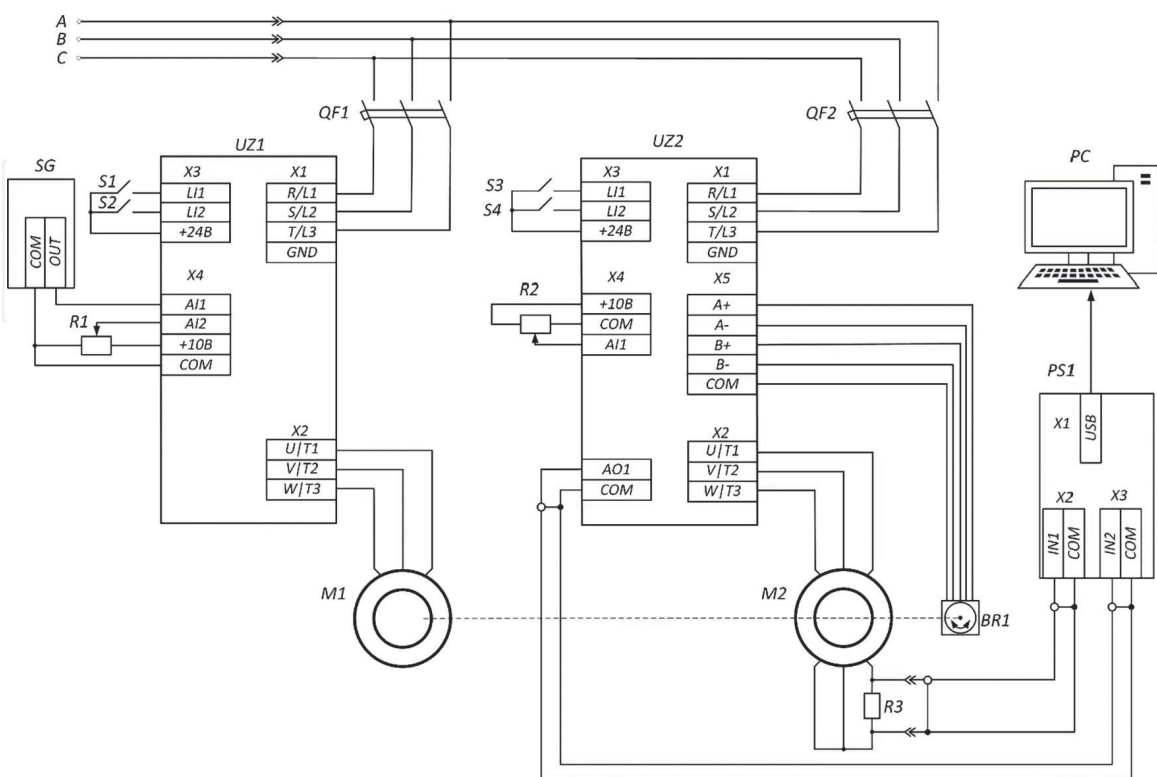
Figure 11.
Stand scheme.
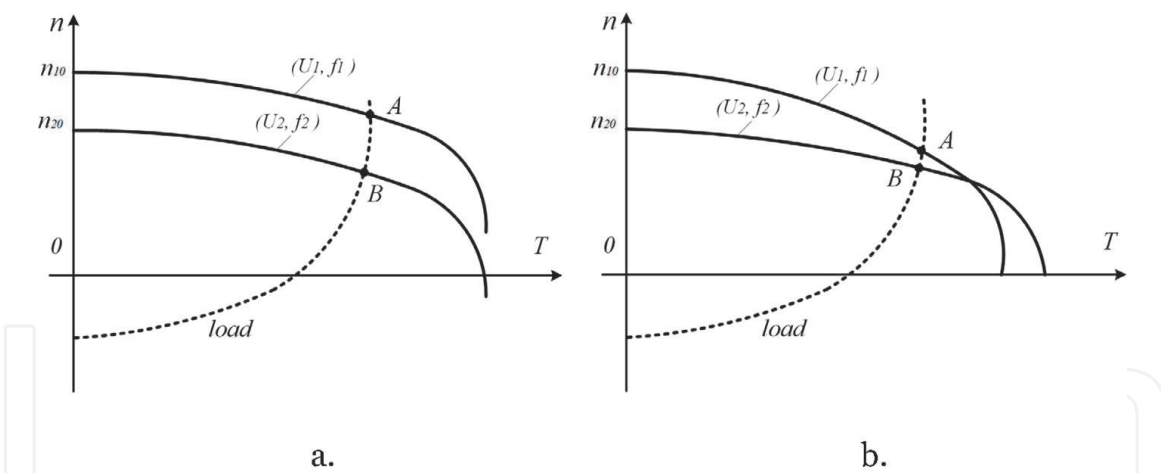
Figure 12.
Mechanical characteristics of the counter activation of the working drive of the stand with different parameters of the stator voltage (U, f) and the load drive. (a) U/f = const. and (b) $\acute{U}_1/f_1 > U_2/f_2$.

As follows from the figures, it is quite difficult to evaluate the efficiency of torque generation in the drive-by one or another control method using these diagrams. Since all these algorithms control the frequency of the stator voltage to a greater or lesser extent, even by the speed signal, it is difficult to estimate the sliding in the motor during experiments.

A methodology was proposed for evaluating the effectiveness of the AED control method by sliding, necessary for the formation of torque in the motor.

Sliding can be determined most accurately in a real drive by the frequency of the rotary current. To work with this technique, the working motor in the stand was replaced with an electric motor with a phase rotor, in which rotor current sensors were installed. **Figures 13** and **14** show diagrams of rotor currents in the working motor of the stand in a circuit with dynamic feedback, and in a circuit with vector control and a PID speed controller, respectively. The results were very telling. The frequency of the main harmonic of the rotor current in the drive with DPF (3.5 Hz) is significantly lower than in the drive with a PID speed controller (8.125 Hz).

In the analysis of the experiments, the main attention was paid to the frequency of rotor current, which is in the circuit with the DPF was significantly lower. But also turned out to be smaller and the amplitude values of the rotor current. To carry out a more detailed assessment of the effectiveness of choice of the stator voltage vector, new experiments were conducted.
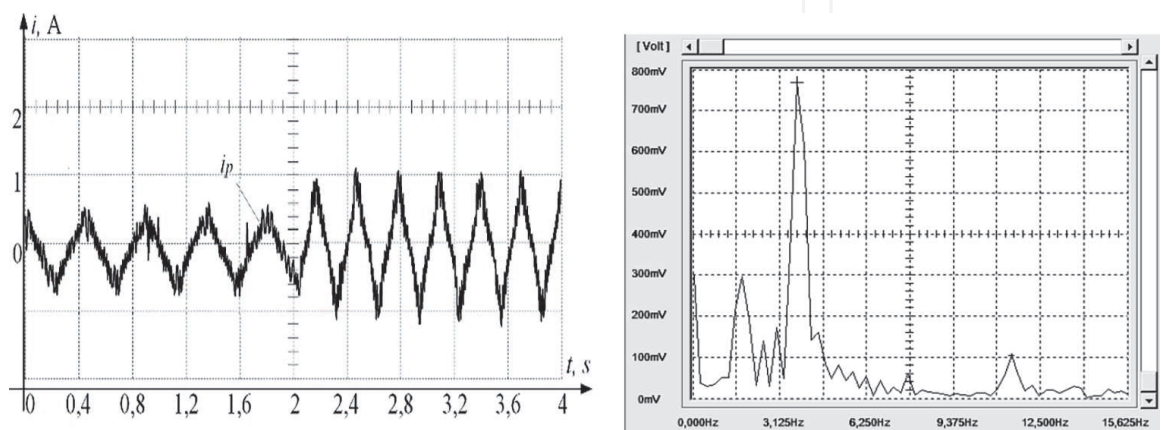
Figure 13.
Rotor currents and the spectrum of rotor current in drive with scalar control and DPF.
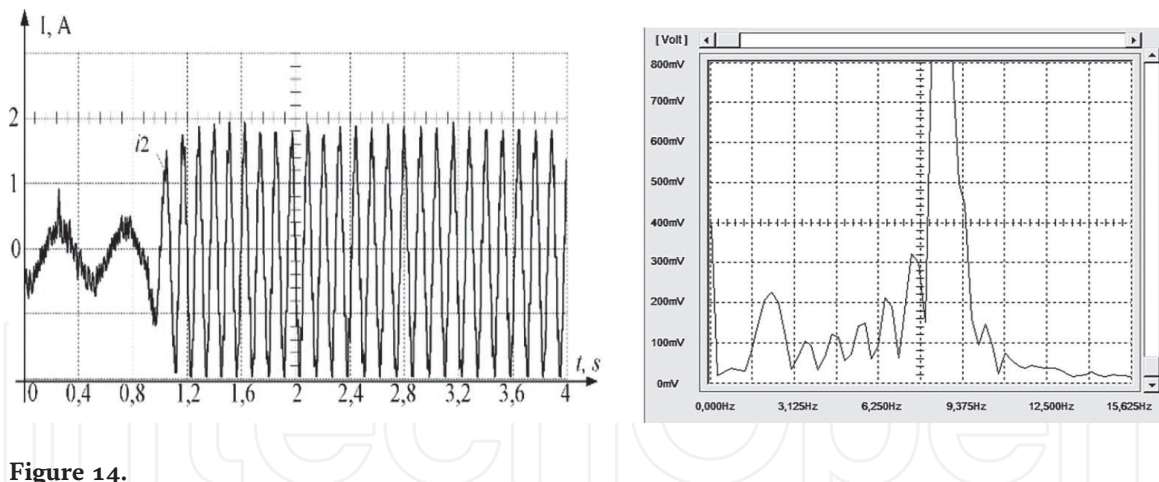
Figure 14.
Rotor currents and the spectrum of rotor current in drive with vector control and speed loop.

3. New experiments with static modes

3.1 Methodology and course of experiments

The working drive, in which five control methods are implemented sequentially, is output at rotational speeds corresponding to the set frequencies of the stator voltage—20 and 30 Hz—**Table 1**.

The load drive generates a braking torque corresponding to the "counter" mechanical characteristic with a given rotational speed of 10 and 15 Hz.

Signals of currents and frequencies are recorded in the rotor and stator of the working drive without load and when switched on with the load drive in steady-state modes. Data in **Tables 1**–**5**.

The values of the voltage U_1, the amplitude of the stator current I_1, the rotation speed recalculated in FC relative to a given frequency are recorded according to the

	F_1, Hz	U_1, V	Fs, Hz	I_1, A	F_2, Hz	I_2, A	F_1	U/f_1
SC	20	91	18.6	0.5	1.5	1.48	20.1	4.5
VC	20	83	18.1	0.4	1.75	1.88	19.85	4.3
SVC	20	90	20	0.39	1.72	1.76	21.76	4.3
DPF	20	92	18.6	0.42	1.42	1.3	20	4.5
DPF2	20	103	19.7	0.36	1.3	1.3	21	4.9

Table 1.
Parameters of the working drive at low load, the load drive is switched off.

	F_1, Hz	U_1, V	Fs, Hz	I_1, A	F_2, Hz	I_2, A	F_1	U/f_1
SC	20	91	6.1	0.7	13.8	12.8	19.9	4.5
VC	20	84	0	0.8	20	15.8	20	4.2
SVC	20	111	11.8	0.7	14.9	14.6	26.7	4.2
DPF	20	103	10.6	0.7	12.2	11.3	22.8	4.6
DPF2	20	110	12.9	0.7	9.6	10	22.5	4.9

Table 2.
Parameters of the working drive at a load of 70% of Mn *(setting the speed of the load drive is equivalent to setting "15 Hz").*

	F_1, Hz	U_1, V	Fs, Hz	I_1, A	F_2, Hz	I_2, A	F_1	U/f_1
SC	30	135	28.8	0.5	1.5	2.1	30.3	4.5
VC	30	135	29	0.5	1.1	2.5	30.1	4.5
DPF	30	134	29	0.5	0.9	2.6	31.6	4.4

Table 3.
Parameters of the working drive at low load, the load drive is switched off.

	F_1, Hz	U_1, V	Fs, Hz	I_1, A	F_2, Hz	I_2, A	F_1	U/f_1
SC	30	138	24.8	0.6	7.5	6.2	32.3	4.2
VC	30	138	24.7	0.6	7.0	7	31.7	4.3
DPF	30	152	28.3	0.6	6.6	6.8	35.1	4.3

Table 4.
Parameters of the working drive at a load of 50% of Mn *(setting the speed of the load drive is equivalent to setting "10 Hz").*

	F_1, Hz	U_1, V	Fs, Hz	I_1, A	F_2, Hz	I_2, A	F_1	U/f_1
SC	30	139	21.6	0.7	10	9.2	31.6	4.4
VC	30	139	21.8	0.7	9	9.2	30.8	4.45
DPF	30	165	29	0.7	9	9.6	38	4.3

Table 5.
Parameters of the working drive at a load of 70% of Mn *(setting the speed of the load drive is equivalent to setting "15 Hz").*

readings of the FC monitor, the rotor current is recorded by the Instek GDS-2062 oscilloscope.

The actual values of the frequency of the stator voltage *Fs* and the ratio U/f_1 in each experiment are calculated from the values of the measured rotational speed and frequency of the rotor current. These relations determine, as indicated in [6, 10], the main magnetic flux in the engine, the value of the critical torque and, according to the Kloss formula, the slip required to create torque in this static mode. The frequency of the rotor currents determines the actual slip in the working drive.

Comment 1: The stator current changes little by increasing the load and the torque of the "working" electric motor—0.5 A—without load, and 0.6–0.7 at during loads, its changes cannot be analyzed. Rotary current varies significantly—from 1.3 to 2.6 A without load and from 6 to 16 A with loads.

It is a rotary current, being active, creates a torque. DPF communication, managing simultaneously and frequency, and voltage—*U/f*, retains its value and the magnitude of the main magnetic flux in the engine, the value of an absolute slip and the amplitude of the rotor currents also change little when the control algorithms change. But the speed of rotation under load is better adjusted than in drives with "open" algorithms. The DPF connection simply "shifts" the mechanical characteristics parallel to natural—**Figure 12a**.

Communication DPF2 increases the *U/f* and at the same time—the main magnetic flux in the motor. The drive currents, sliding and the reactive power flows are reduced, as compared with the electric drive with DPF—**Figure 12b** and **Tables 6** and 7. Since these control algorithms are formed, as seen from the tables, different stator voltage vectors to establish a clear connection between the control algorithm,

F_1, Hz	U_1, V	Fs, Hz	I_1, A	F_2, Hz	I_2, A	F_1	U/f$_1$
30	137	28.4	0.432	1.695	1.8	30.1	4.6
30	150	28.6	0.472	1.351	1.88	29.95	5
30	180	29.3	0.576	0.9	1.76	30.2	6
30	200	29.6	0.680	0.75	1.72	30.35	6.8
30							

Table 6.
Parameters of the working drive at light load with only scalar control, the load drive is off.

F_1, Hz	U_1, V	Fs, Hz	I_1, A	F_2, Hz	I_2, A	F_1	U/f$_1$
30	137	24	0.480	5.8	5.8	29.8	4.6
30	150	25.2	0.496	5	5.44	30.6	5
30	180	26.7	0.600	3.3	5.12	30	6
30	200	27.4	0.680	2.63	4.48	30	6.8

Table 7.
Parameters of the working drive with only scalar control, at a load of 50% of Mn (setting the speed of the load drive is equivalent to setting "10 Hz").

this vector and the drive mode at loads, that is, values of currents and their frequencies have been carried out in additional experiments.

Additional experiments were carried out in the following order.

In the scalar control mode, a different amplitude of the stator voltage from 130 to 200 V was set for a certain rotation frequency. All process parameters in the stator and rotor were recorded at low load (**Table 6**). The parameters of the processes in the drives when the load drive is turned on, rotating in the opposite direction, are given in **Table 7**.

Comment 2: The analysis showed that when the amplitude and frequency of the voltage across the motor stator are set similar to the parameters of the "selected" DPF and DPF2 modes, the parameters of the processes in the rotor and stator turn out to be the same with scalar control.

At the maximum value of *U/f* = 6.8, the minimum values of the rotor current (1.72 A) and slip (4.48 Hz) under load, and 0.75 A and 2.63 Hz, respectively, at low load are fixed.

This confirms the assumption that it is the parameters of the stator voltage (*U*, *f*), which determine the main magnetic flux in the motor, that determine the operating mode of the AED—sliding and rotor currents. The larger the main flow, the smaller the slip and the rotor current.

The control algorithms (SC, SVC, DPF, and DPF2) only "select" the values of *U* and *f* according to the task for the rotation speed, the load torque and in accordance with the control algorithm.

The DPF control algorithm relies on a continuous nonlinear transfer function—a more accurate interpretation of the AED, since it does not have the assumptions that are made in vector control (only the main harmonics in the currents and EMF of the motor, $\omega_1 = \omega$, $\frac{d\psi_2}{dt} = 0$), "selects" control more efficiently.

This correction method is certainly more promising both for static and quasi-static modes, and for operation under complex disturbances and in complex technological systems (special vehicles, wind turbines, drones, technological complexes, power engineering …).

3.2 The discussion of the results

As experiments have shown, the static modes of operation of the AED, given U and f, can be accurately described by vector diagrams and mechanical characteristics. At the same time, it is necessary to clarify the amount of slip required to create torque.

The "selection" of the values of the amplitude and frequency of the stator voltage is carried out by the control algorithm—SC, SVC, and DPF. With an increase in the main flux in the motor, the stator current at low load increases, while the rotor current and slip at high load fall. That is, positive torque feedback provides low no-load stator currents and reduced rotor currents under load.

Traditional control algorithms (SC, SVC) do not choose U and f optimally, since the algorithms are based on vector equations and several assumptions that are very erroneous for working under load even in static modes ($\omega_1 = \omega$, for example). The control transition paths are selected incorrectly.

The use of continuous nonlinear transfer functions interpreting AED and corrections by local feedbacks on these functions form transition processes (including transition trajectories) in complex operating modes with variable load.

This determines their advantages and prospects for the use of continuous transfer functions and continuous local corrections and structures in AED complex technological complexes.

This is especially important because, in terms of price, reliability and overload capacity, AED has no alternatives.

3.3 About vector control

Theoretical "understanding" of vector control problems shows that sequential correction, which is vector control (**Figure 3**) with simplifications of the original equations, passing through nonlinear blocks with delays (the pulsed power part of the FC) is very inefficient and experiments confirm this, although statics is closest to the original vector equations. We should expect even greater problems in operating modes with significant dynamics of loads and rotational speeds. The sequential correction that vector control "tries" to implement does not work, because it is based on many erroneous simplifications and is ineffective as a sequential correction of the nonlinear structure of torque generation in asynchronous motors.

3.4 About direct torque control (DTC) technology

Over 30 years of direct torque control (DTC) technology, a lot of work has been devoted. An example of the scheme is shown in **Figure 15**.

Most often, there are no detailed descriptions, there is no technology, including the characteristics of the "observer" of flow coupling—its accuracy, dynamics, which fundamentally affect all processes. Another obvious, but ignored in the descriptions of technology, the problem is the presence of high harmonics in all. This "suggests" some kind of conditionality of the results.

The very appearance of this kind of vector control is probably a reaction to the poor-quality operation of the vector control at the entrance from the torque of the disturbance and represents the formation of a transition trajectory from one vector state to another, improved compared to the vector transition, in which this trajectory is not paid attention at all. The trajectory is carried out at the expense of "basic" vectors. The algorithm software is very complex and other companies (except ABB) do not use it. Confirms that discontinuous vector control does not give trajectories of transitions from one state to another.

Figure 15.
Block diagram of direct torque control (DTC) in an asynchronous electric drive.

On the speed of the formation of the torque, which is often mentioned in the description of technology [21–24]. The transition time is 1–2 ms without specifying the drive power and specific charts are difficult to consider a convincing argument. In the article [21] the increasing time of 50 ms is also fast, but already real. In our experiments (**Figure 10a**) The process of recovery of speed is 80–100 ms. That for the torque commensurate with DTC. It is implemented in any FC and has prospects for improvement.

It should be noted that in the articles to directly control the torque [21–24] there are no at least some mathematics of the description of the dynamics—differential equations, etc.

On local connections based on the representation of an asynchronous electric motor by a nonlinear transfer function.

The transfer function of the link forms the torque in an asynchronous electric motor—the initial and adjusted ones are determined by the transition conditions, that is, the initial and final conditions for changing the load and frequency of the stator voltage.

The continuity of the transfer function contributes to optimizing the formation of the transition trajectory from one state to another. With the original vector equations, this transition is not determined and an additional algorithm is required—not only the basic vectors, but also the trajectories of transitions to them.

Since in all experiments, that is, at different operating speeds and loads with a deep positive connection in the stator current (more precisely, in the developed torque of the sliding value), the amplitudes of the currents are smaller than with traditional control methods (scalar and vector), it can be reasonably argued that the amplification of the main magnetic flux in asynchronous motors reduces the angle of shift between the reduced vectors of the rotor and stator currents of the motor.

4. Conclusion

The static modes of operation of the AEP in the control methods under consideration are described fairly accurately by nonlinear transfer functions (NTF), but transitions between static states are described incorrectly in these algorithms and

when loading the work of these algorithms—in closed vector circuits—is incorrect and leads to significantly inefficient modes.

The local connection formed by the NTF is a positive dynamic feedback, "selects" the parameters of the stator voltage (U, f) the best for parrying static disturbing torques.

Discontinuous vector AED equations, based on which correction algorithms are formed by traditional methods, do not allow to obtain optimal modes of parrying load surges with their help.

The advantages in the quality of operation of control systems using the proposed local connections are even more obvious with large variable external disturbances and when working in complex ACS.

There is a proposal to introduce into the drive a positive feedback by the amplitude of the rotor current, as an analogue of the feedback by torque.

The operation of AED in complex systems and under complex disturbing influences is not described in principle (with sufficient accuracy) by the method of vector equations, hence the endless modes of selection and calculation of engine and drive parameters, automatic identification, and, finally, DTC technology.

Feedback by the torque or by the value of the active current of the stator under load reduces the currents of the stator, rotor and slip, that is, makes the processes more active, which is extremely "useful" for drives with large and varying loads.

Author details

Vladimir L. Kodkin*, Alexandr S. Anikin, Alexandr A. Baldenkov
and Natalia A. Loginova
South Ural State University, Chelyabinsk, Russian Federation

*Address all correspondence to: kodkina2@mail.ru

IntechOpen

References

[1] Usoltsev AA. Vector Control of Asynchronous Motors: Tutorial. Spb.: ITMO; 2002. p. 120. Available from: http://servomotors.ru/documentation/frequency_control_of_asynchronous_motors/chastupr.pdf

[2] Park R, Robertson B. The reactances of synchronous machines. Transactions of the American Institute of Electrical Engineers. 1928;**47**(2):514-535

[3] Vas P. Vector Control of AC Machines. New York, NY, USA: Oxford University Press; 1990

[4] Mishchenko VA. The vector control method of electromechanical converters. Electrical Engineering. 2004;**7**:47-51

[5] Kodkin VL, Anikin AS, Baldenkov AA. Identification of AC drivers from the families of frequency characteristics. Russian Electrical Engineering. 2020;**91**(12):756-760. DOI: 10.3103/S1068371220120081

[6] Kodkin V, Anikin A. On the physical nature of frequency control problems of induction motor drives. Energies. 2021;**14**(14):4246. DOI: 10.3390/en14144246

[7] Kodkin VL, Anikin AS, Baldenkov AA. The dynamics identification of asynchronous electric drives via frequency response. International Journal of Power Electronics and Drive Systems. 2019;**10**(1):66-73. DOI: 10.11591/ijpeds.v10n1.pp66-73

[8] Kodkin VL, Anikin AS. Experimental study of the VFD's speed stabilization efficiency under torque disturbances. International Journal of Power Electronics and Drive Systems. 2021;**12**(1):80-87. DOI: 10.11591/ijpeds.v12.i1.pp80-87

[9] Kodkin V, Baldenkov A, Anikin A. A method for assessing the stability of digital automatic control systems (ACS) with discrete elements. Hypothesis and simulation results. Energies. 2021;**14**(20):6561. DOI: 10.3390/en14206561

[10] Kodkin VL, Anikin AS, Baldenkov AA. Stabilization of the stator and rotor flux linkage of the induction motor in the asynchronous electric drives with frequency regulation. International Journal of Power Electronics and Drive Systems. 2020;**11**(1):213-219. DOI: 10.11591/ijpeds.v11.i1.pp213-219

[11] Codkin VL, Anikin AS, Baldenkov AA. Assessing the efficiency of control systems of asynchronous electric drives using spectral analysis of rotor currents. Russian Electrical Engineering. 2021;**92**(1):32-37. DOI: 10.3103/S1068371221010065

[12] Kodkin VL, Anikin AS, Shmarin YA. Dynamic load disturbance correction for alternative current electric drives. In: 2016 2nd International Conference on Industrial Engineering, Applications and Manufacturing (ICIEAM): Proceedings: South Ural State University (National Research University), Chelyabinsk, Russia. 2016. DOI:10.1109/SIBCON.2015.7146978

[13] Kodkin VL. Methods of optimizing the speed and accuracy of optical complex guidance systems based on equivalence of automatic control system domain of attraction and unconditional stability of their equivalent circuits. In: Proceedings of SPIE—The International Society for Optical Engineering. 2016

[14] Kodkin VL, Anikin AS. Frequency control of asynchronous electric drives in transport. In: 2015 International Siberian Conference on Control and Communications (SIBCON 2015)—Proceedings. 2015. DOI: 10.1109/SIBCON.2015.7146978

[15] Kodkin VL, Anikin AS, Shmarin YA. Effective frequency control for

induction electric drives under overloading. Russian Electrical Engineering. 2014;**85**(10):641-644. DOI: 10.3103/S1068371214100101

[16] Kodkin VL, Anikin AS, Baldenkov AA. Experimental research of asynchronous electric drive with positive dynamic feedback on stator current. In: 2017 International Conference on Industrial Engineering, Applications and Manufacturing (ICIEAM)—Proceedings. 2017. DOI:10.1109/ICIEAM.2017.8076179

[17] Kodkin VL, Anikin AS, Baldenkov AA. Spectral analysis of rotor currents in frequency-controlled electric drives. In: 2nd International Conference on Automation, Mechanical and Electrical Engineering (AMEE 2017)—Proceedings. 2017. DOI: 10.2991/amee-17.2017.26

[18] Kodkin VL, Anikin AS, Baldenkov AA. Families of frequency characteristics, as a basis for the identification of asynchronous electric drives. In: 2018 International Russian Automation Conference (RusAutoCon). 2018

[19] Kodkin VL, Anikin AS, Baldenkov AA. Analysis of stability of electric drives as non-linear systems according to Popov criterion adjusted to amplitude and phase frequency characteristics of its elements. In: 2nd International Conference on Applied Mathematics, Simulation and Modelling (AMSM 2017)—Proceedings. 2017. pp. 7-14. DOI: 10.12783/dtetr/amsm2017/14810

[20] Kodkin VL, Anikin AS, Baldenkov AA. The analysis of the quality of the frequency control of induction motor carried out on the basis of the processes in the rotor circuit. Journal of Physics Conference Series. 2018;**944**(1):012052

[21] Karandeev DY, Engel EA. Direct torque control of an induction motor using adaptive neurocontroller in conditions of uncertainty. Internet Journal Science. 2015;**7**(5):1-9. DOI: 10.15862/91TVN515

[22] Wang F et al. Advanced control strategies of induction machine: Field oriented control, direct torque control and model predictive control. Energies. 2018;**11**(1):120. DOI: 10.3390/en11010120

[23] Alsofyani IM, Idris NRN. Simple flux regulation for improving state estimation at very low and zero speed of a speed sensorless direct torque control of an induction motor. IEEE Transactions on Power Electronics. 2016;**31**(4):3027-3035. DOI: 10.1109/TPEL.2015.2447731

[24] Toufouti R. Direct torque control for induction motor using intelligent techniques. Journal of Theoretical and Applied Information Technology. 2007;**3**(3):35-44